

Energy levels and magnetic dipole transition parameters for the nitrogen isoelectronic sequence

Mu-Hong Hu(胡木宏), Nan Wang(王楠), Pin-Jun Ouyang(欧阳品均), Xin-Jie Feng(冯新杰), Yang Yang(杨扬), and Chen-Sheng Wu(武晨晟)

Citation: Chin. Phys. B, 2022, 31 (**9**): 093101. DOI: 10.1088/1674-1056/ac7a12
Journal homepage: http://cpb.iphy.ac.cn; http://iopscience.iop.org/cpb

What follows is a list of articles you may be interested in

Energy levels and transition data of $3p^6 3d^8$ and $3p^5 3d^9$ configurations in Fe-like ions (Z = 57, 60, 62, 64, 65)

Bao-Ling Shi(施宝玲), Yi Qin(秦毅), Xiang-Fu Li(李向富), Bang-Lin Deng(邓邦林), Gang Jiang(蒋刚), and Xi-Long Dou(豆喜龙)

Chin. Phys. B, 2022, 31 (**5**): 053102. DOI: 10.1088/1674-1056/ac4480

Spectroscopy and scattering matrices with nitrogen atom: Rydberg states and optical oscillator strengths

Yuhao Zhu(朱宇豪), Rui Jin(金锐), Yong Wu(吴勇), and Jianguo Wang(王建国)

Chin. Phys. B, 2022, 31 (**4**): 043103. DOI: 10.1088/1674-1056/ac1f05

Transition parameters of Li-like ions (Z=7-11) in dense plasmas

Xiang-Fu Li(李向富), Li-Ping Jia(贾利平), Hong-Bin Wang(王宏斌), and Gang Jiang(蒋刚)

Chin. Phys. B, 2021, 30 (**5**): 053102. DOI: 10.1088/1674-1056/abea80

Effect of Sm doping into $CuInTe_2$ on cohesive energy before and after light absorption

Tai Wang(王泰), Yong-Quan Guo(郭永权), and Cong Wang(王聪)

Chin. Phys. B, 2021, 30 (**4**): 043101. DOI: 10.1088/1674-1056/abd167

Analytical expressions of non-relativistic static multipole polarizabilities for hydrogen-like ions

Xuesong Mei(梅雪松), Wanping Zhou(周挽平), Zhenxiang Zhong(钟振祥), Haoxue Qiao(乔豪学)

Chin. Phys. B, 2020, 29 (**4**): 043101. DOI: 10.1088/1674-1056/ab75d0

DATA PAPER

Energy levels and magnetic dipole transition parameters for the nitrogen isoelectronic sequence

Mu-Hong Hu(胡木宏)[1,†], Nan Wang(王楠)[1], Pin-Jun Ouyang(欧阳品均)[1], Xin-Jie Feng(冯新杰)[1], Yang Yang(杨扬)[1], and Chen-Sheng Wu(武晨晟)[2,‡]

[1] *School of Physics and Electronic Technology, Liaoning Normal University, Dalian* 116029, *China*
[2] *Institute of Applied Physics and Computational Mathematics, Beijing* 100094, *China*

(Received 31 March 2022; revised manuscript received 30 May 2022; accepted manuscript online 18 June 2022)

Theoretical calculations of the energy levels and magnetic dipole transition parameters for the $1s^22s^22p^3$ and $1s^22p^5$ configurations of nitrogen isoelectronic sequence with $Z = 21$–30 are performed using multi-congfiguration Dirac–Fock (MCDF) method. Based on the relativistic computational code GRASP2k compiled within the framework of MCDF method, the electron correlations, Breit interaction and QED effects are well treated in detail. The energy levels, line strengths and transition rates of magnetic dipole transition are obtained and compared with the experimental data available. For most cases, good agreements are achieved and the relative differences of them are less than 0.114% , 8.43% and 9.80%, respectively. The scaling laws of the fine structure splitting and transition rate are obtained on the isoelectronic sequence and the corresponding physical mechanisms are discussed. The data sets for tables are openly available at https://www.doi.org/10.57760/sciencedb.j00113.00022.

Keywords: energy level, magnetic dipole transition, transition rate, scaling law, nitrogen-like ions, multi-congfiguration Dirac–Fock (MCDF) method

PACS: 31.15.V–, 31.15.ve, 31.15.vj, 32.70.Cs **DOI:** 10.1088/1674-1056/ac7a12

1. Introduction

The growing demands of spectra data for highly charged nitrogen-like ions along isoelectronic sequence, such as energy levels, radiative transition wavelengths, line strength and transition rates, have become urgent in astrophysics. The reliable data can motivate the further analysis of the observed spectra containing the information about structure, physical conditions, chemical abundances and transition region of astrophysical objects.[1–6] On the other hand, a wide comparison among the high-resolution spectra obtained from various astrophysical sources shows that most part of the emission and absorption lines are generated from iron ions, including the Fe XX ion, the nitrogen-like ion studied mostly.[7–10] It is unquestionable that the thoughtful analysis and modeling on these spectra are very helpful in profound comprehension of astrophysical sources' structure, feature and processes of evolution. The reliable spectra data of nitrogen-like ions also play significant roles in the field of plasma diagnostics.[11–13] In many cases, it is difficult to obtain plasma parameters directly, accurate and abundant spectra data can provide valuable reference for research on characters of plasma, such as electron temperature, electron density distribution and influence from environmental and operation conditions. Moreover, accurate spectra data are important not only for distinguishing the blending lines emitted in collisionally ionized plasma but also for understanding the spectra lines produced in photoionized plasma.

During the past decades, the great comprehensive theoretical research on highly charged many-electron system has been employed, a great deal of valuable atomic basic data of nitrogen-like ions have been obtained with different methods. At the first stage, the electric dipole (E1), electronic quadrupole (E2) and magnetic dipole (M1) transitions of nitrogen-like ions with $Z = 10$–30 between $2s^22p^3$, $2p^4$ and $2p^5$ configurations have been investigated with the stationary second-order many-body perturbation theory (MBPT), in which the relativistic corrections are considered in the Breit–Pauli approximation.[14,15] With the development of the iron project, atomic data for Fe XX including the energy levels, oscillator strengths, line strengths and radiative transition rates of dipole allowed and forbidden transitions are presented with the multiconfiguration Dirac–Fock (MCDF) method and the relativistic Breit–Pauli *R*-matrix (RBPR) method, respectively.[16,17] The computations on wavelength and oscillator strength of transitions from $1s^22s^22p^23s$, $1s^22s^22p^23d$, $1s^22s^12p^33p$ configurations to $1s^22s^22p^3$ configuration in Fe XX ion are also performed using the configuration interaction Dirac–Fock and Dirac–Fock–Sturm method.[18] The results mentioned above have limited precision and cannot accommodate the special demands of observations. In response to the advances in measurements, energies and transition properties for states of $2s^22p^3$, $2p^4$ and $2p^5$ configurations in nitrogen-

†Corresponding author. E-mail: humuhong@163.com
‡Corresponding author. E-mail: 251538424@qq.com

© 2022 Chinese Physical Society and IOP Publishing Ltd

like ions are evaluated with the relativistic configuration interaction (RCI) method and extensive multi-configuration Dirac–Hartree–Fock (MCDHF) method.[19,20] As for $2l^5$ and $1s2l^43l'$ configurations, energies with high accuracy are predicted with a combination of RCI method and MBPT method in FAC code, and complete and consistent sets of energies and transition parameters involving the $n = 3$, 4 levels in nitrogen-like ions are given with the same method as an in-depth research.[21,22] However, the research on nitrogen-like isoelectronic sequence is not satisfying at all, the results of energy level structure and transition property calculated previously are not accurate to meet the special requirements[23] and the results obtained latter are not complete. In addition, the research on scaling laws along the isoelectronic sequence has attracted more attention because of their regularities and practicalities.[24,25] The scaling laws describe the relationship between the energy levels, transition rates, line ratios and the nuclear charge Z, they also reveal the competitions of physical interactions in different procedures. Therefor, it is significant to carry out research on scaling laws, which contain more detail of dynamical processes and also provide an efficient way to obtain other values interested via interpolation method.

Among the various theoretical methods and numerical techniques used to carry out approximate computation, MCDF method has made considerable progresses to meet the increasing demands of different calculations, its approximation of the calculation on atomic stationary states and transitions is described in detail in the literature and not repeated here.[26–29] MCDF method has become more and more important in higher precision calculation. In general, it is indispensable to accomplish the accurate study on energy structure and property of radiative transition without efficient program. Based on the MCDF method, GRASP program is a convenient program provided to perform rigorous calculations on energy levels and transition properties, in which the relativistic effects and electron correlation effect are taken into account adequately. GRASP has been used in a wide range of applications since its public release, its reliability and accuracy have been verified with a large amount of results obtained.[30–35] In this work, we apply the MCDF method to study $1s^22s^22p^3$ and $1s^22p^5$ configurations for nitrogen-like ions with $Z = 21$–30, the energy level structures, transition rates and line strengths of 19 M1 transitions for $2s^22p^3$and $2p^5$ configurations along the isoelectronic sequence are computed systematically. With these theoretical results, the scaling laws of the fine structure splitting and transition rates in isoelectronic sequence are analyzed, and interesting features of isoelectronic sequence are explained.

2. Theory

The present calculation was carried out in the framework of the fully relativistic MCDF method with the implementation of GRASP2K package, it was presented in detail by Grant.[36,37] In this method, the relativistic Hamiltonian for a system with N electrons in atomic units is defined as

$$H_{\rm DC} = \sum_{i}^{N}\left[c\boldsymbol{\alpha}_i\cdot\boldsymbol{p}_i + (\beta_i - 1)c^2 + V_i^{\rm N}\right] + \sum_{i>j}^{N} 1/r_{ij}, \tag{1}$$

where $V_i^{\rm N}$ is the Coulomb interaction between the nucleus and the ith electron. The atomic state wave function (ASF) for a given state with parity P, total angular momentum J and its component along z direction M_J can be described by a linear combination of configuration wave function (CSF) having the same P, J, M_J, it reads

$$|\Psi(PJM_J)\rangle = \sum_{i=1}^{N_{\rm c}} c_i\,|\Phi(\gamma_i PJM_J)\rangle. \tag{2}$$

Here $N_{\rm c}$ is the number of configuration wave function, c_i is the mixing coefficient determined by optimizing the energy expectation value of the relativistic Hamiltonian, γ_i represents other labels required to specify the configuration state wavefunction. The configuration state wavefunctions acted as basis sets are anti-symmetrized linear combinations of products of relativistic orbitals, in which the radial orbitals can be optimized via the extended optimal level (EOL) scheme used in the self-consistent field (SCF) method. For highly charged ions, quantum electrodynamics (QED) effect and transverse photon interaction play important roles in accurate calculations. Therefore, the leader QED effects including the vacuum polarization generated by charge distribution and electron self-energy are taken into account using a perturbation approximation and expressed as follows:[38]

$$H_{rr}^{\rm VP} = \sum_{a=1}^{n_w} q_r(a)\int_0^{\infty} {\rm d}rV^{\rm VP}(r)(P_{n_a\kappa_a}^2(r) + Q_{n_a\kappa_a}^2(r)), \tag{3}$$

$$H_{rr}^{\rm SE} = \sum_{a=1}^{n_w} q(r)E_{n_a\kappa_a}^{\rm SE}. \tag{4}$$

As for the transverse photon interaction, its low-frequency limit named as Breit interaction can be expressed as

$$H_{\rm Breit} = -\frac{1}{2r_{ij}}\left[\boldsymbol{\alpha}_i\cdot\boldsymbol{\alpha}_j + \frac{(\boldsymbol{\alpha}_i\cdot\boldsymbol{r}_{ij})(\boldsymbol{\alpha}_j\cdot\boldsymbol{r}_{ij})}{r_{ij}^2}\right]. \tag{5}$$

Based on the atomic state wavefunction, the transition parameters, such as transition rate, line strength and weighted oscillator strength, for a multipole transition from state J to state J' are all related into the reduced transition matrix element

$$\left\langle \Psi(PJ)\left\|\boldsymbol{O}^{(K)}\right\|\Psi(P'J')\right\rangle, \tag{6}$$

where $\boldsymbol{O}^{(K)}$ is the relevant transition operator of rank K, electronic multipoles and magnetic multipoles are designated with $K = 1$ and $K = 0$, respectively. As far as the present study concerned, M1 transitions are the main objective targeted.

3. Results and discussion

The electron correlation effect plays very important role in theoretical calculations of atomic structure and transition property. However, due to the complex interactions and convergence difficulties encountered in SFC calculation, it is a challenging task to apply a reliable method to guarantee the accuracy of evaluation on electron correlation effect of many-body atomic system. In order to obtain the CSFs with manageable size and most crucial correlations, the active space (AS) approach was adopted in present work, it can be executed with three steps. Firstly, the 1s and 2s orbitals of ground configuration $2s^22p^3$ and excited configuration $2p^5$ in nitrogen-like isoelectronic sequence ($Z = 21$–30) were fixed, the calculations were performed without any correlations since both orbitals were regarded as an inactive core. Then the orbital set was expended to all $n = 3$ orbitals, all CSFs generated by single and double excitation (SD) from two configurations to available orbitals were included in this expansion. After that, the $n = 3$ orbitals expanded with fixed core orbitals were optimized simultaneously through the EOL scheme. The low-frequency limit Breit interaction, vacuum polarization and the self-energy corrections were calculated using the RCI method after the optimization. Similar processes were continued until the orbitals were extended to $n = 8$. In these processes, the size of the orbitals for the SD excitation was enlarged rapidly with the adding of additional layer of orbitals. In order to maintain the enough size of orbitals and resolve the problem of convergence accompanied in the expansion, the optimizing was employed only on the orbitals added while the previous orbitals were fixed simultaneously. The number of CSFs in every expansion for each J of $2s^22p^3$ and $2p^5$ configurations in nitrogen-like isoelectronic sequence can be controlled in a reasonable and efficient region with this time-saving optimization. As an example, the energy levels of $2s^22p^3$ and $2p^5$ configurations for Sc XV ion are listed in Table 1. The active space models with SD excitation were labeled with different notations nSD, $n = 3$, 4, 5, 6, 7, 8. It can be found that the behavior of convergence for energy is excellent although the number of CSF increases rapidly. In contrast to other lower spin states, energy of high spin state $^4S_{2/3}$ tends to converge more quickly.

Table 1. Energies of $2s^22p^3$ and $2p^5$ configurations for Sc XV ion with different active spaces of orbitals (in a.u.).

Model	N_c	$1s^22s^22p^3$					$1s^22p^5$	
		$^4S^\circ_{3/2}$	$^2D^\circ_{3/2}$	$^2D^\circ_{5/2}$	$^2P^\circ_{1/2}$	$^2P^\circ_{3/2}$	$^2P^\circ_{3/2}$	$^2P^\circ_{1/2}$
3SD	1164	–633.4402201	–632.9250104	–632.8757314	–632.5896542	–632.5188786	–626.8527287	–626.6680906
4SD	5707	–633.4845244	–632.9712519	–632.9222575	–632.6337760	–632.5632781	–626.9017015	–626.7168068
5SD	15353	–633.4936491	–632.9822710	–632.9332384	–632.6450933	–632.5745115	–626.9149907	–626.7300667
6SD	31760	–633.4971904	–632.9865235	–632.9374685	–632.6495019	–632.5788778	–626.9199279	–626.7349920
7SD	56586	–633.4989343	–632.9885967	–632.9395292	–632.6516595	–632.5810129	–626.9222961	–626.7373541
8SD	91489	–633.4999216	–632.9897589	–632.9406836	–632.6528716	–632.5822119	–626.9236150	–626.7386694

There are seven states with $J = 5/2, 3/2, 1/2$ in $2s^22p^3$ and $2p^5$ configurations, the energy levels of nitrogen-like ions with $Z = 21$–30 computed in current work are presented as E_{cal} in Table 2. In comparison, some theoretical results and observed data from National Institute of Standard and Technology (NIST) named as E_{MCDHF}, E_{RCI} and E_{NIST} are also listed in Table 2.[18,19,39] The comparing between the theoretical results and observed data shows that the results of RCI method are the most accurate so far. In most cases, the results of present work agree well with the data of NIST and the range of relative differences is smaller than that of the relative difference of Ref. [23].

For majority of ions in the isoelectronic sequence, the fine structure splittings calculated in present work are consistent with the experimental values,[39] all the relative differences are within 0.9%, the differences range from 3.3 cm^{-1} to 280 cm^{-1}. The largest difference appears in $^2P_{3/2,1/2}$ state of $2p^5$ configuration for Zn XXIV ion, the fine structure splitting calculated in present work, RCI method and observed in experiment are 205020 cm^{-1}, 204995 cm^{-1} and 205900 cm^{-1}, respectively. The theoretical results agree well with each other, both of them have similar deviations from the observation, the discrepancy of present work amounts to 880 cm^{-1}, the discrepancy of RCI method is a little bigger, it is 905 cm^{-1}.

The relationships between the fine structure splittings of $^2D_{5/2,3/2}$, $^2P_{3/2,1/2}$ states from $2s^22p^3$ configuration, $^2P_{1/2,3/2}$ states from $2p^5$configuration and nuclear charge Z are plotted in Fig. 1. The solid dots are results computed in this work, the lines in different color represent the results of scaling laws fitted in different Z region. For $2s^22p^3$ $^2D_{5/2,3/2}$ states shown in Fig. 1(a), the fine structure splitting is small and increases smoothly in the lower Z area, it tends to increase slowly at about $Z = 28$. In the low Z area with $Z < 28$, the fine structure splitting can be scaled with $Z_{eff}^{4.1}$, where $Z_{eff} = Z$–6, and in the high Z area with $Z > 28$, it is scaled with $Z_{eff}^{1.5}$. The variation of the scaling law reveals an interesting fact, namely, the electron spin–orbit interaction is dominant in the low Z area, however, the effect of electron–electron Coulomb interaction in $^2D_{5/2,3/2}$ states tends to be strong enough and to be predominant in the competition between the electron–electron

Coulomb interaction and spin–orbit interaction with the increase of Z. For $2s^22p^3\ ^2P_{3/2,1/2}$ states given in Fig. 1(b), the variation of fine structure splitting in the isoelectronic sequence is not as obvious as that of $^2D_{5/2,3/2}$ states. The scaling law can be simply scaled by $Z_{\rm eff}^{4.8}$ in low Z area and $Z_{\rm eff}^{4.2}$ in high Z area. As for $2p^5\ ^2P_{1/2,3/2}$ states given in Fig. 1(c), the fine structure splitting varies a little fast along the isoelectronic sequence, which can be scaled by $Z_{\rm eff}^{3.4}$ in low Z area and $Z_{\rm eff}^{3.7}$ in high Z area. Both variations of scaling laws indicate that the spin–orbit interaction tends to be more dominant in the whole region of Z. Therefore, the variations of scale laws imply the competition between the electron–electron Coulomb interaction and spin–orbit interaction along the isoelectronic sequence.

There is great interesting in research on property of spectra for M1 transition because of its peculiarity in all possible transitions, which is known as forbidden transition in dipole radiation because of the same parity of the initial state and final state. M1 transitions are observed mainly in emission and described quantitatively with transition rate, therefore, the accuracy of transition energy and line strength is crucial to implement theoretical study on transition process. The transition energy is much more reliable because of its strong sensitivity on the wavefunction, in which the thoughtful consideration of electron correlations, Breit interaction and QED effects is regarded as an essential ingredient of accurate calculation. With the well-behaved wavefunction, the line strength and transition rate of 19 M1 transitions among all levels of $2s^22p^3$ and $2p^5$ configurations for nitrogen-like ions with $Z = 21$–30 are evaluated and given in Table 3, some NIST data of line strength in literature and transition rate[40] are also collected in the table. Almost all the results of line strength differ from NIST within 8.53% excluding the $2s^22p^3\ ^2D_{3/2} \rightarrow\ ^2D_{5/2}$ transition in Ni XXII, as the largest discrepancy, it is about 10.63%. As for the transition rate, the discrepancy is within 9.80%, and it tends to decrease slowly in the isoelectronic sequence.

Table 2. Energy levels of $2s^22p^3$ and $2p^5$ configurations for nitrogen-like isoelectronic systems with $Z = 21$–30 (in $\rm cm^{-1}$).

Ion	Results	$1s^22s^22p^3$					$1s^22p^5$	
		$^4S^\circ_{3/2}$	$^2D^\circ_{3/2}$	$^2D^\circ_{5/2}$	$^2P^\circ_{1/2}$	$^2P^\circ_{3/2}$	$^2P^\circ_{3/2}$	$^2P^\circ_{1/2}$
Sc XV	$E_{\rm Cal.}$	0	111966.41	122737.05	185903.71	201411.53	1443314.78	1483905.15
	$E_{\rm RCI}$[19]	0	111360	122104	185056	200626	1442074	1482551
	$E_{\rm NIST}$[39]	0	111200	121960	184840	200450	1441710	1482190
Ti XVI	$E_{\rm Cal.}$	0	116930.53	131554.6	198875.8	220336.4	1539647.71	1589845.22
	$E_{\rm RCI}$[19]	0	116299	130937	197982	219525	1538117	1588320
	$E_{\rm NIST}$[39]	0	116030	130720	197700	219250	1537660	1587830
V XVII	$E_{\rm Cal.}$	0	121827.14	141127.82	212630.9	241595.55	1638500.68	1700089.8
	$E_{\rm RCI}$[19]	0	121191	140517	211731	240791	1636934	1698530
	$E_{\rm NIST}$[39]	0	120930	140260	211420	240500	1636530	1698100
Cr XVIII	$E_{\rm Cal.}$	0	126945.32	151677.42	227443.39	265665.08	1740582.29	1815416.94
	$E_{\rm MCDHF}$[18]	0	126328	151075	226546	264860	1738860	1813685
	$E_{\rm RCI}$[19]	0	126326	151079	226544	264870	1738998	1813840
	$E_{\rm NIST}$[39]	0	126060	150810	226180	264540	1738700	1813560
Mn XIX	$E_{\rm Cal.}$	0	132642.75	163489.61	243604.78	293052.92	1846403.82	1936534.14
	$E_{\rm RCI}$[19]	0	132048	162907	242711	292273	1844801	1934938
	$E_{\rm NIST}$[39]	0	131770	162450	242110	291730	1844360	1934390
Fe XX	$E_{\rm Cal.}$	0	139377.63	176904.48	261459.5	324326.84	1956537.92	2064221.21
	$E_{\rm RCI}$[19]	0	138818	176342	260577	323566	1954921	2062609
	$E_{\rm NIST}$[39]	0	138620	176130	260270	323340	1954310	2061990
Co XXI	$E_{\rm Cal.}$	0	147696.82	192310.58	281400	360111.18	2071617.28	2199329.67
	$E_{\rm RCI}$[19]	0	147183	191774	280534	359374	2069990	2197703
	$E_{\rm NIST}$[39]	0	147040	191530	280260	359000	2069550	2197070
Ni XXII	$E_{\rm Cal.}$	0	158206.77	210130.92	303852.82	401073.95	2192321.27	2342769.21
	$E_{\rm MCDHF}$[18]	0	1575732	209602	302989	400330	2190414	2340835
	$E_{\rm RCI}$[19]	0	157747	209623	303007	400361	2190686	2341128
	$E_{\rm NIST}$[39]	0	157536	209380	302600	400100	2190300	2340900
Cu XXIII	$E_{\rm Cal.}$	0	171530.8	230802.06	329257.63	447906.84	2319352.31	2495484.62
	$E_{\rm RCI}$[19]	0	171132	230324	328433	447217	2317711	2493829
	$E_{\rm NIST}$[39]	0	170860	230070	327900	446780	2316720	2492890
Zn XXIV	$E_{\rm Cal.}$	0	188262.86	254751.18	358044.27	501302.73	2453421.69	2658441.66
	$E_{\rm MCDHF}$[18]	0	187907	254278	357220	500593	2451454	2656422
	$E_{\rm RCI}$[19]	0	187926	254303	357241	500633	2451770	2656765
	$E_{\rm NIST}$[39]	0	188130	254110	357130	501140	2451700	2657600

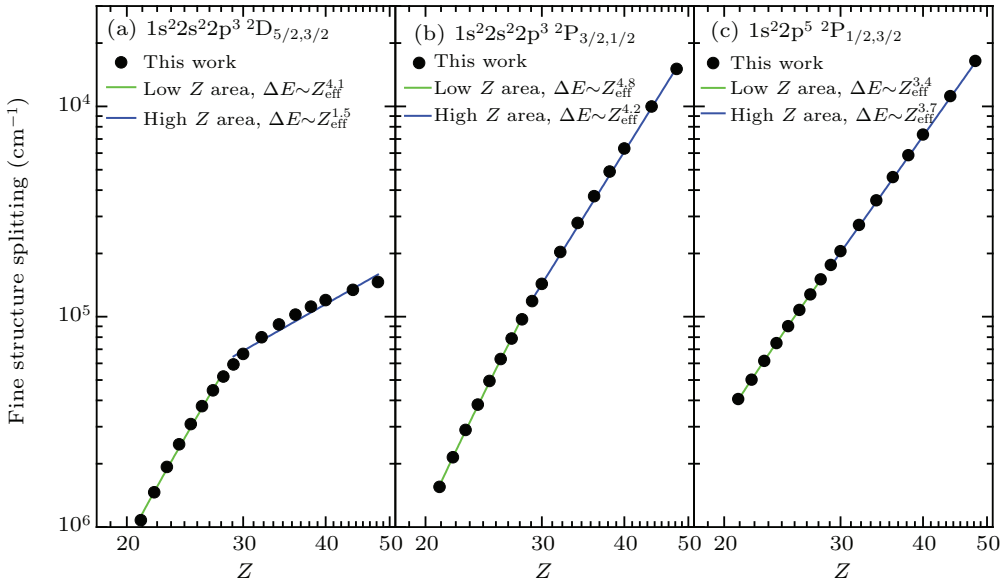


Fig. 1. The relationship between the fine structure splitting of $2s^22p^3\ ^2P_{3/2,1/2}$, $^2D_{5/2,3/2}$, $2p^5\ ^2P_{1/2,3/2}$ states in nitrogen-like isoelectronic sequence and the nuclear charge Z.

Table 3. The line strength S and transition rate A for all possible M1 transitions of nitrogen-like ions (Z = 21–30), the number in square brackets represents the power of 10.

Transition	Sc XV				Ti XVI			
	S	$S_{\rm NIST}$[40]	A	$A_{\rm NIST}$[40]	S	$S_{\rm NIST}$[40]	A	$A_{\rm NIST}$[40]
$2p^5\ ^2P_{1/2} \rightarrow 2s^22p^3\ ^2P_{1/2}$	2.174[−11]		6.413[−4]		2.497[−11]		9.064[−4]	
$2s^22p^3\ ^2P_{3/2} \rightarrow 2s^22p^3\ ^2P_{1/2}$	1.125[0]	1.100[0]	2.828[1]	2.82[1]	1.089[0]	1.100[0]	7.256[1]	7.2[1]
$2p^5\ ^2P_{3/2} \rightarrow 2s^22p^3\ ^2P_{1/2}$	2.370[−5]		3.177[2]		3.141[−5]		5.106[2]	
$2s^22p^3\ ^2P_{1/2} \rightarrow 2s^22p^3\ ^4S_{3/2}$	3.222[−2]	3.522[−2]	2.793[3]	3.000[3]	4.406[−2]	4.700[−2]	4.674[3]	4.9[3]
$2p^5\ ^2P_{1/2} \rightarrow 2s^22p^3\ ^4S_{3/2}$	5.398[−6]		2.379[2]		6.576[−6]		3.564[2]	
$2s^22p^3\ ^2P_{1/2} \rightarrow 2s^22p^3\ ^2D_{3/2}$	1.733[−1]	1.857[−1]	9.445[2]	1.000[3]	1.969[−1]	2.200[−1]	1.462[3]	1.6[3]
$2p^5\ ^2P_{1/2} \rightarrow 2s^22p^3\ ^2D_{3/2}$	1.801[−6]		6.273[1]		1.563[−6]		6.735[1]	
$2p^5\ ^2P_{1/2} \rightarrow 2s^22p^3\ ^2P_{3/2}$	3.904[−5]		1.111[3]		5.296[−5]		1.835[3]	
$2p^5\ ^2P_{1/2} \rightarrow 2p^5\ ^2P_{3/2}$	1.330[0]	1.386[0]	1.200[3]	1.240[3]	1.3308[0]	1.330[0]	2.269[3]	2.27[3]
$2s^22p^3\ ^2D_{3/2} \rightarrow 2s^22p^3\ ^4S_{3/2}$	1.004[−1]	1.186[−1]	9.505[2]	1.100[3]	1.707[−1]	1.900[−1]	1.840[3]	2.0[3]
$2s^22p^3\ ^2P_{3/2} \rightarrow 2s^22p^3\ ^4S_{3/2}$	9.021[−2]	9.390[−2]	4.970[3]	5.100[3]	1.044[−1]	1.100[−1]	7.529[3]	7.8[3]
$2p^5\ ^2P_{3/2} \rightarrow 2s^22p^3\ ^4S_{3/2}$	3.992[−5]		8.093[2]		5.056[−5]		1.244[3]	
$2s^22p^3\ ^2P_{3/2} \rightarrow 2s^22p^3\ ^2D_{3/2}$	5.498[−1]	6.049[−1]	2.653[3]	2.900[3]	6.412[−1]	7.000[−1]	4.781[3]	5.2[3]
$2p^5\ ^2P_{3/2} \rightarrow 2s^22p^3\ ^2D_{3/2}$	4.457[−5]		7.093[2]		6.056[−5]		1.176[3]	
$2p^5\ ^2P_{3/2} \rightarrow 2s^22p^3\ ^2P_{3/2}$	2.52[−6]		3.266[1]		3.689[−6]		5.712[1]	
$2s^22p^3\ ^2D_{5/2} \rightarrow 2s^22p^3\ ^4S_{3/2}$	3.623[−3]		3.012[1]		6.881[−3]		7.043[1]	
$2s^22p^3\ ^2D_{5/2} \rightarrow 2s^22p^3\ ^2D_{3/2}$	2.065[0]	2.020[0]	1.160[1]	1.13[1]	2.008[0]	1.970[0]	2.823[1]	2.81[1]
$2s^22p^3\ ^2P_{3/2} \rightarrow 2s^22p^3\ ^2D_{5/2}$	3.296[−1]	3.680[−1]	1.083[3]	1.200[3]	3.835[−1]	4.300[−1]	1.810[3]	2.0[3]
$2p^5\ ^2P_{3/2} \rightarrow 2s^22p^3\ ^2D_{5/2}$	2.394[−5]		3.719[2]		3.156[−5]		5.942[2]	
Transition	V XVII				Cr XVIII			
	S	$S_{\rm NIST}$[40]	A	$A_{\rm NIST}$[40]	S	$S_{\rm NIST}$[40]	A	$A_{\rm NIST}$[40]
$2p^5\ ^2P_{1/2} \rightarrow 2s^22p^3\ ^2P_{1/2}$	2.809[−11]		1.247[−3]		3.101[−11]		1.675[−3]	
$2s^22p^3\ ^2P_{3/2} \rightarrow 2s^22p^3\ ^2P_{1/2}$	1.053[0]	1.030[0]	1.725[2]	1.71[2]	1.019[0]	1.000[0]	3.837[2]	3.82[2]
$2p^5\ ^2P_{3/2} \rightarrow 2s^22p^3\ ^2P_{1/2}$	4.108[−5]		8.031[2]		5.287[−5]		1.235[3]	
$2s^22p^3\ ^2P_{1/2} \rightarrow 2s^22p^3\ ^4S_{3/2}$	5.934[−2]	6.400[−2]	7.694[3]	8.2[3]	7.857[−2]	8.300[−2]	1.247[4]	1.3[4]
$2p^5\ ^2P_{1/2} \rightarrow 2s^22p^3\ ^4S_{3/2}$	7.808[−6]		5.175[2]		9.032[−6]		7.288[2]	
$2s^22p^3\ ^2P_{1/2} \rightarrow 2s^22p^3\ ^2D_{3/2}$	2.171[−1]	2.400[−1]	2.192[3]	2.4[3]	2.312[−1]	2.500[−1]	3.165[3]	3.4[3]
$2p^5\ ^2P_{1/2} \rightarrow 2s^22p^3\ ^2D_{3/2}$	1.230[−6]		6.522[1]		8.511[−7]		5.525[1]	
$2p^5\ ^2P_{1/2} \rightarrow 2s^22p^3\ ^2P_{3/2}$	7.066[−5]		2.957[3]		9.248[−5]		4.642[3]	
$2p^5\ ^2P_{1/2} \rightarrow 2p^5\ ^2P_{3/2}$	1.329[0]	1.360[0]	4.189[3]	4.29[3]	1.329[0]	1.300[0]	7.512[3]	7.6[3]
$2s^22p^3\ ^2D_{3/2} \rightarrow 2s^22p^3\ ^4S_{3/2}$	2.721[−1]	3.000[−1]	3.318[3]	3.6[3]	4.164[−1]	4.500[−1]	5.745[3]	6.1[3]
$2s^22p^3\ ^2P_{3/2} \rightarrow 2s^22p^3\ ^4S_{3/2}$	1.171[−1]	1.200[−1]	1.114[4]	1.1[4]	1.261[−1]	1.300[−1]	1.594[4]	1.6[4]
$2p^5\ ^2P_{3/2} \rightarrow 2s^22p^3\ ^4S_{3/2}$	6.260[−5]		1.857[3]		7.522[−5]		2.675[3]	
$2s^22p^3\ ^2P_{3/2} \rightarrow 2s^22p^3\ ^2D_{3/2}$	7.344[−1]	7.800[−1]	8.508[3]	9.0[3]	8.278[−1]	8.900[−1]	1.490[4]	1.6[4]
$2p^5\ ^2P_{3/2} \rightarrow 2s^22p^3\ ^2D_{3/2}$	8.182[−5]		1.925[3]		1.098[−4]		3.111[3]	
$2p^5\ ^2P_{3/2} \rightarrow 2s^22p^3\ ^2P_{3/2}$	5.160[−6]		9.486[1]		6.906[−6]		1.494[2]	
$2s^22p^3\ ^2D_{5/2} \rightarrow 2s^22p^3\ ^4S_{3/2}$	1.200[−2]	1.200[−2]	1.516[2]	1.5[2]	2.013[−2]	2.100[−2]	3.159[2]	3.2[2]
$2s^22p^3\ ^2D_{5/2} \rightarrow 2s^22p^3\ ^2D_{3/2}$	1.950[0]	1.900[0]	6.304[1]	6.2[1]	1.895[0]	1.860[0]	1.289[2]	1.27[2]
$2s^22p^3\ ^2P_{3/2} \rightarrow 2s^22p^3\ ^2D_{5/2}$	4.356[−1]	4.900[−1]	2.979[3]	3.3[3]	4.829[−1]	5.200[−1]	4.823[3]	5.2[3]
$2p^5\ ^2P_{3/2} \rightarrow 2s^22p^3\ ^2D_{5/2}$	4.108[−5]		9.302[2]		5.267[−5]		1.425[3]	

Table 3. (*Continued*).

Transition	Mn XIX				Fe XX			
	S	$S_{\rm NIST}$[40]	A	$A_{\rm NIST}$[40]	S	$S_{\rm NIST}$[40]	A	$A_{\rm NIST}$[40]
$2p^5\ ^2P_{1/2} \rightarrow 2s^22p^3\ ^2P_{1/2}$	3.373[−11]		2.208[−3]		3.614[−11]		2.856[−3]	
$2s^22p^3\ ^2P_{3/2} \rightarrow 2s^22p^3\ ^2P_{1/2}$	9.877[−1]	9.7[−1]	8.0546[2]	8.0[2]	9.591[−1]	9.457[−1]	1.607[3]	1.600[3]
$2p^5\ ^2P_{3/2} \rightarrow 2s^22p^3\ ^2P_{1/2}$	6.705[−5]		1.862[3]		8.388[−5]		2.755[3]	
$2s^22p^3\ ^2P_{1/2} \rightarrow 2s^22p^3\ ^4S_{3/2}$	1.022[−1]	1.1[−1]	1.993[4]	2.1[4]	1.304[−1]	1.400[−1]	3.144[4]	3.3[4]
$2p^5\ ^2P_{1/2} \rightarrow 2s^22p^3\ ^4S_{3/2}$	1.018[−5]		9.969[2]		1.117[−5]		1.325[3]	
$2s^22p^3\ ^2P_{1/2} \rightarrow 2s^22p^3\ ^2D_{3/2}$	2.385[−1]	2.5[−1]	4.394[3]	4.5[3]	2.384[−1]	2.512[−1]	5.851[3]	6.100[3]
$2p^5\ ^2P_{1/2} \rightarrow 2s^22p^3\ ^2D_{3/2}$	4.828[−7]		3.822[1]		1.871[−7]		1.799[1]	
$2p^5\ ^2P_{1/2} \rightarrow 2s^22p^3\ ^2P_{3/2}$	1.189[−4]		7.119[3]		1.505[−4]		1.069[4]	
$2p^5\ ^2P_{1/2} \rightarrow 2p^5\ ^2P_{3/2}$	1.329[0]	1.33[0]	1.312[4]	1.31[4]	1.328[0]	1.330[0]	2.237[4]	2.24[4]
$2s^22p^3\ ^2D_{3/2} \rightarrow 2s^22p^3\ ^4S_{3/2}$	6.116[−1]	6.5[−1]	9.625[3]	1.0[4]	8.611[−1]	8.900[−1]	1.572[4]	1.6[4]
$2s^22p^3\ ^2P_{3/2} \rightarrow 2s^22p^3\ ^4S_{3/2}$	1.299[−1]	1.3[−1]	2.205[4]	2.2e+04	1.280[−1]	1.280[−1]	2.946[4]	2.91[4]
$2p^5\ ^2P_{3/2} \rightarrow 2s^22p^3\ ^4S_{3/2}$	8.754[−5]		3.716[3]		9.851[−5]		4.975[3]	
$2s^22p^3\ ^2P_{3/2} \rightarrow 2s^22p^3\ ^2D_{3/2}$	9.220[−1]	9.8[−1]	2.566[4]	2.7[4]	1.018[0]	1.060[0]	4.342[4]	4.49[4]
$2p^5\ ^2P_{3/2} \rightarrow 2s^22p^3\ ^2D_{3/2}$	1.463[−4]		4.967[3]		1.935[−4]		7.828[3]	
$2p^5\ ^2P_{3/2} \rightarrow 2s^22p^3\ ^2P_{3/2}$	8.887[−6]		2.246[2]		1.105[−5]		3.240[2]	
$2s^22p^3\ ^2D_{5/2} \rightarrow 2s^22p^3\ ^4S_{3/2}$	3.246[−2]	3.4[−2]	6.377[2]	6.6[2]	5.017[−2]	5.17[−2]	1.249[3]	1.27[3]
$2s^22p^3\ ^2D_{5/2} \rightarrow 2s^22p^3\ ^2D_{3/2}$	1.840[0]	1.82[0]	2.429[2]	2.36[2]	1.786[0]	1.760[0]	4.244[2]	4.17[2]
$2s^22p^3\ ^2P_{3/2} \rightarrow 2s^22p^3\ ^2D_{5/2}$	5.247[−1]	5.6[−1]	7.696[3]	8.2[3]	5.607[−1]	5.900[−1]	1.212[4]	1.27[4]
$2p^5\ ^2P_{3/2} \rightarrow 2s^22p^3\ ^2D_{5/2}$	6.656[−5]		2.207[3]		8.301[−5]		3.155[3]	
Transition	Co XXI				Ni XII			
	S	$S_{\rm NIST}$[40]	A	$A_{\rm NIST}$[40]	S	$S_{\rm NIST}$[40]	A	$A_{\rm NIST}$[40]
$2p^5\ ^2P_{1/2} \rightarrow 2s^22p^3\ ^2P_{1/2}$	3.830[−11]		3.645[−3]		4.021[−11]		4.597[−3]	
$2s^22p^3\ ^2P_{3/2} \rightarrow 2s^22p^3\ ^2P_{1/2}$	9.331[−1]	9.100[−1]	3.069[3]	3.0[3]	9.097[−1]	9.120[−1]	5.634[3]	5.700[3]
$2p^5\ ^2P_{3/2} \rightarrow 2s^22p^3\ ^2P_{1/2}$	1.036[−4]		4.008[3]		1.264[−4]		5.741[3]	
$2s^22p^3\ ^2P_{1/2} \rightarrow 2s^22p^3\ ^4S_{3/2}$	1.630[−1]	1.700[−1]	4.8984[4]	5.0[4]	1.991[−1]	2.100[−1]	7.531[4]	7.8[4]
$2p^5\ ^2P_{1/2} \rightarrow 2s^22p^3\ ^4S_{3/2}$	1.194[−5]		1.713[3]		1.242[−5]		2.154[3]	
$2s^22p^3\ ^2P_{1/2} \rightarrow 2s^22p^3\ ^2D_{3/2}$	2.313[−1]	2.400[−1]	7.458[3]	7.6[3]	2.182[−1]	2.186[−1]	9.091[3]	9.000[3]
$2p^5\ ^2P_{1/2} \rightarrow 2s^22p^3\ ^2D_{3/2}$	2.083[−8]		2.427[0]		2.507[−8]		3.526[0]	
$2p^5\ ^2P_{1/2} \rightarrow 2s^22p^3\ ^2P_{3/2}$	1.877[−4]		1.575[4]		2.309[−4]		2.280[4]	
$2p^5\ ^2P_{1/2} \rightarrow 2p^5\ ^2P_{3/2}$	1.328[0]	1.330[0]	3.730[4]	3.72[4]	1.327[0]	1.300[0]	6.095[4]	6.0[4]
$2s^22p^3\ ^2D_{3/2} \rightarrow 2s^22p^3\ ^4S_{3/2}$	1.160[0]	1.200[0]	2.521[4]	2.6[4]	1.494[0]	1.600[0]	3.989[4]	4.2[4]
$2s^22p^3\ ^2P_{3/2} \rightarrow 2s^22p^3\ ^4S_{3/2}$	1.206[−1]	1.200[−1]	3.797[4]	3.7[4]	1.085[−1]	1.100[−1]	4.719[4]	4.8[4]
$2p^5\ ^2P_{3/2} \rightarrow 2s^22p^3\ ^4S_{3/2}$	1.070[−4]		6.418[3]		1.123[−4]		7.979[3]	
$2s^22p^3\ ^2P_{3/2} \rightarrow 2s^22p^3\ ^2D_{3/2}$	1.115[0]	1.200[0]	7.204[4]	7.7[4]	1.212[0]	1.200[0]	1.171[5]	1.2[5]
$2p^5\ ^2P_{3/2} \rightarrow 2s^22p^3\ ^2D_{3/2}$	2.532[−4]		1.216[4]		3.273[−4]		1.8587[4]	
$2p^5\ ^2P_{3/2} \rightarrow 2s^22p^3\ ^2P_{3/2}$	1.333[−5]		4.506[2]		1.565[−5]		6.067[2]	
$2s^22p^3\ ^2D_{5/2} \rightarrow 2s^22p^3\ ^4S_{3/2}$	7.421[−2]	7.600[−2]	2.373[3]	2.4[3]	1.049[−1]	1.100[−1]	4.375[3]	4.5[3]
$2s^22p^3\ ^2D_{5/2} \rightarrow 2s^22p^3\ ^2D_{3/2}$	1.732[0]	1.700[0]	6.9142]	6.7[2]	1.676[0]	1.660[0]	1.055[3]	1.04[3]
$2s^22p^3\ ^2P_{3/2} \rightarrow 2s^22p^3\ ^2D_{5/2}$	5.912[−1]	6.300[−1]	1.884[4]	2.0[4]	6.164[−1]	6.400[−1]	2.894[4]	3.0[4]
$2p^5\ ^2P_{3/2} \rightarrow 2s^22p^3\ ^2D_{5/2}$	1.022[−4]		4.577[3]		1.245[−4]		6.538[3]	
Transition	Cu XXIII				Zn XXIV			
	S	$S_{\rm NIST}$[40]	A	$A_{\rm NIST}$[40]	S	$S_{\rm NIST}$[40]	A	$A_{\rm NIST}$[40]
$2p^5\ ^2P_{1/2} \rightarrow 2s^22p^3\ ^2P_{1/2}$	4.182[−11]		5.734[−3]		4.323[−11]		7.098[−3]	
$2s^22p^3\ ^2P_{3/2} \rightarrow 2s^22p^3\ ^2P_{1/2}$	8.887[−1]		1.001[4]		8.697[−1]		1.724[4]	
$2p^5\ ^2P_{3/2} \rightarrow 2s^22p^3\ ^2P_{1/2}$	1.525[−4]		8.108[3]		1.821[−4]		1.130[4]	
$2s^22p^3\ ^2P_{1/2} \rightarrow 2s^22p^3\ ^4S_{3/2}$	2.373[−1]		1.143[5]		2.76279[−1]		1.710[5]	
$2p^5\ ^2P_{1/2} \rightarrow 2s^22p^3\ ^4S_{3/2}$	1.260[−5]		2.641[3]		1.248[−5]		3.163[3]	
$2s^22p^3\ ^2P_{1/2} \rightarrow 2s^22p^3\ ^2D_{3/2}$	2.004[−1]		1.060[4]		1.798[−1]		1.187[4]	
$2p^5\ ^2P_{1/2} \rightarrow 2s^22p^3\ ^2D_{3/2}$	2.141[−7]		3.624[1]		5.712[−7]		1.161[2]	
$2p^5\ ^2P_{1/2} \rightarrow 2s^22p^3\ ^2P_{3/2}$	2.806[−4]		3.249[4]		3.370[−4]		4.563[4]	
$2p^5\ ^2P_{1/2} \rightarrow 2p^5\ ^2P_{3/2}$	1.323[0]		9.776[4]		1.326[0]		1.541[5]	
$2s^22p^3\ ^2D_{3/2} \rightarrow 2s^22p^3\ ^4S_{3/2}$	1.838[0]	1.90[0]	6.255[4]	6.40[4]	2.166[0]		9.745[4]	
$2s^22p^3\ ^2P_{3/2} \rightarrow 2s^22p^3\ ^4S_{3/2}$	9.342[−2]		5.661[4]		7.732[−2]		6.568[4]	
$2p^5\ ^2P_{3/2} \rightarrow 2s^22p^3\ ^4S_{3/2}$	1.138[−4]		9.577[3]		1.118[−4]		1.114[4]	
$2s^22p^3\ ^2P_{3/2} \rightarrow 2s^22p^3\ ^2D_{3/2}$	1.3093[0]		1.864[5]		1.403[0]		2.902[5]	
$2p^5\ ^2P_{3/2} \rightarrow 2s^22p^3\ ^2D_{3/2}$	4.170[−4]		2.787[4]		5.229[−4]		4.098[4]	
$2p^5\ ^2P_{3/2} \rightarrow 2s^22p^3\ ^2P_{3/2}$	1.796[−5]		7.939[2]		2.019[−5]		1.0137[3]	
$2s^22p^3\ ^2D_{5/2} \rightarrow 2s^22p^3\ ^4S_{3/2}$	1.413[−1]	1.46[−1]	7.828[3]	7.98[3]	1.826[−1]		1.357[4]	
$2s^22p^3\ ^2D_{5/2} \rightarrow 2s^22p^3\ ^2D_{3/2}$	1.618[0]	1.60[0]	1.515[3]	1.49[3]	1.560[0]		2.062[0]	
$2s^22p^3\ ^2P_{3/2} \rightarrow 2s^22p^3\ ^2D_{5/2}$	6.370[−1]		4.396[4]		6.536[−1]		6.606[4]	
$2p^5\ ^2P_{3/2} \rightarrow 2s^22p^3\ ^2D_{5/2}$	1.499[−4]		9.211[3]		1.787[−4]		1.281[4]	

The transitions rates from excited states $2p^5\ ^2P_{1/2,3/2}$ to the lowest state $2s^22p^3\ ^4S_{3/2}$ in nitrogen-like isoelectronic sequence are illustrated in Fig. 2. Both transition rates have the same behavior, they increase fast in low Z area, and tend to increase slowly in high Z area. The transition rate of $^2P_{1/2} \rightarrow {}^4S_{3/2}$ can be scaled by $Z_{\rm eff}^{5.98}$ in low Z area and $Z_{\rm eff}^{2.82}$ in high Z area, and the transition rate of $^2P_{3/2} \rightarrow {}^4S_{3/2}$ follows the scaling laws of $Z_{\rm eff}^{6.34}$ in low Z area and $Z_{\rm eff}^{1.55}$ in high Z area. It can be inferred that the scaling laws of transition rates are adjusted due to the changes of electron–electron Coulomb interactions and spin–orbital interactions. In low Z region, the energy level separation is primarily caused by the spin–orbital interactions. While the increases of transition rates tend to slow down in high Z region because of the domination of the electron–electron Coulomb interactions, which leads to energy level separation.[41]

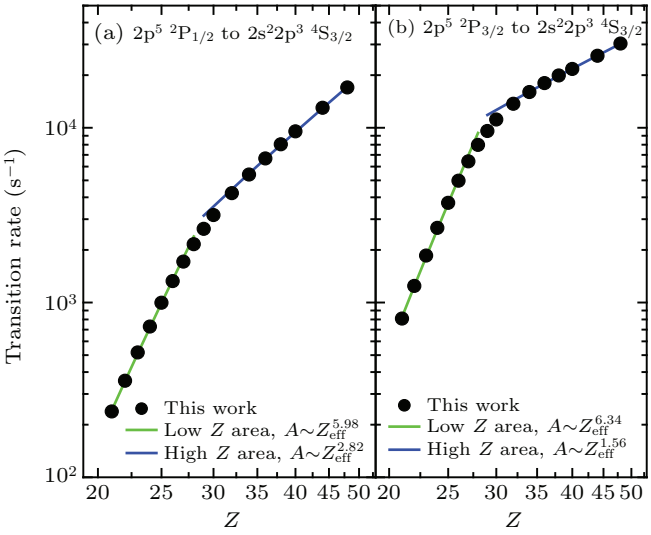


Fig. 2. The transitions rates from excited states $2p^5\ ^2P_{1/2,3/2}$ to the lowest state $2s^22p^3\ ^4S_{3/2}$ in nitrogen-like isoelectronic sequence.

4. Conclusion

In this work, the energy levels and M1 transition properties for the $1s^22s^22p^3$ and $1s^22p^5$ configurations of nitrogen-like isoelectronic sequence ($Z = 21$–30) are investigated with the MCDF method. In the present work, the electron correlation effects on the energy level and transition rates are well treated with a large configuration space applied in the CI calculation. For the isoelectronic sequence, the contributions of Breit interaction and QED effects tend to increase gradually, which is essential to accomplish accurate calculation. Then, good agreements are achieved for the energy levels, line strength and transition rate in comparison with the available experimental and theoretical results with the Breit interaction and QED effects included. The dependence of fine structure splitting and transition rate on nuclear charge is achieved and discussed. It is found that the scaling laws of fine structure splitting and transition rate change along isoelectronic sequence because of the competition between the electron–electron Coulomb interactions and spin–orbital interactions. The atomic number of nitrogen-like ions corresponding to the changing of scaling laws is foretasted approximately and the adjustment of scaling laws involved is analyzed.

Combined with the good observations, some transition parameters can provide much information for density diagnosis of planetary nebulas or the inner corona, and some results of highly charged nitrogen-like ions are needed in fusion plasma. The atomic data and scaling laws studied in present work are hoped to be useful to predict reliable indications of astrophysics studies and plasma diagnosis.

Data availability

The data that support the findings of this study are openly available in Science Data Bank at https://www.doi.org/10.57760/sciencedb.j00113.00022.

Acknowledgement

Project supported by the National Natural Science Foundation of China (Grant No. 12175096)

References

[1] Kallman T R and Palmeri P 2007 *Rev. Mod. Phys.* **79** 79
[2] Massacrier G and Artru M C 2012 *Astronomy & Astrophysics* **538** A52
[3] Del Zanna G and Woods T N 2013 *Astronomy & Astrophysics* **555** A59
[4] Beiersdorfer P, Träbert E, Lepson J K, Brickhouse N S and Golub L 2014 *The Astrophysical Journal* **25** 788
[5] Träbert E, Beiersdorfer P, Brickhouse N S and Golub L 2014a *The Astrophysical Journal Supplement Series* **6** 215
[6] Träbert E, Beiersdorfer P, Brickhouse N S and Golub L 2014b *The Astrophysical Journal Supplement Series* **14** 211
[7] Canizares C R, *et al*. 2000 *The Astrophysical Journal* **539** L41
[8] Brinkman A C, *et al*. 2001 *Astronomy & Astrophysics* **365** L324
[9] Smith R K, Brickhouse N S, Liedahl D A and Raymond J C 2001 *The Astrophysical Journal* **556** L91
[10] Desai P, *et al*. 2005 *The Astrophysical Journal* **625** L59
[11] Seaton M J 1968 *Advances In Atomic Molecular Physics* **4** 331
[12] Sudkewer S 1981 *Physica Scripta* **23** 72
[13] Mohan A, Landi E 2003 *Atomic Data and Nuclear Data Tables* **85** 317
[14] Merkelis G, Vilkas M J, Kisielius R, Gaigalas G and Martinson I 1997 *Physica Scripta* **56** 41
[15] Merkelis G, Martinson I, Kisielius R and Vilkas M J 1999 *Physica Scripta* **59** 122
[16] Nahar S N 2004 *Astronomy & Astrophysics* **413** 779
[17] Jonauskas V, Bogdanovich P and Keenan F P 2005 *Astronomy & Astrophysics* **433** 745
[18] Kotochigova S, Linnik M, Kirby K P and Brickhouse N S 2010 *The Astrophysical Journal Supplement Series* **186** 85
[19] Rynkun P, Jönsson P, Gaigalas G and Froese Fischer C 2014 *Atomic Data and Nuclear Data Tables* **100** 315
[20] Radžiūtė L, Ekman J, Jönsson P and Gaigalas G 2015 *Astronomy & Astrophysics* **582** A61
[21] Gu M F 2005 *The Astrophysical Journal Supplement Series* **156** 105
[22] Wang K, Si R, Dang W, Jönsson P, Guo X L, Li S, Chen Z B, Zhang H, Long F Y, Liu H T, Li D. F, Hutton R, Chen C Y and Yan J 2016 *The Astrophysical Journal Supplement Series* **223** 3
[23] Wang W Y 1992 *Acta Phys. Sin.* **41** 726 (in Chinese)
[24] Gao X, Han X Y, Zeng D L, Jin R and Li J M 2014 *Phys. Lett. A* **378** 1515
[25] Han X Y, Gao X, Zeng D L, Jin R, Yan J, Li J M 2014 *Phys. Rev. A* **89** 042514
[26] Kim Y K and Desclaux J P 1976 *Phys. Rev. Lett.* **36** 139

[27] Cheng K T, Kim Y K and Desclaux J P 1979 *Atomic Data and Nuclear Data Tables* **24** 111
[28] Fischer C F, Brage T and Jonsson P 1997 *Computational Atomic Structure: An MCHF Approach* (Bristol: Institute of Physics Publishing)
[29] Dong C Z, Xie L Y, Zhou X X, Ma X W and Fritzsche S 2003 *Hyperfine Interact* **146/147** 161
[30] Dietrich D D, Leavitt J A, Bashkin S, Conway J G, Gould H M, Donald D, Marrus R, Johnson B M and Pegg D J 1977 *Phys. Rev.* **18** 208
[31] Dyall K G, Grant I P, Johnson C T, Parpia F A and Plummer E P 1989 *Computer Physics Communications* **55** 425
[32] Ding X B, Koike F, Murakami I, Kato D, Sakaue H A, Dong C Z, Nakamura N, Komatsu A and Sakoda J 2011 *J. Phys. B: Atom. Mol. Opt. Phys.* **44** 145004
[33] Ding X, Sun R, Koike F, Kato D, Murakami I, Sakaue H A and Dong C Z 2017 *Euro. Phys. J. D* **71** 73
[34] Liu J P, Li C B and Zou H X 2017 *Chin. Phys. B* **26** 103210
[35] Ding X B, Sun R, Liu J X, Koike F, Murakami I, Kato D, Sakaue H A, Nakamura N and Dong C Z 2017 *J. Phys. B: Atom. Mol. Opt. Phys.* **50** 045004
[36] Grant I P 2007 *Relativistic Quantum Theory of Atoms and Molecules* (Berlin: Springer)
[37] Jonsson P, He X, Froese F C and Grant I P 2007 *Computer Physics Communications* **177** 597
[38] Dyall K G, Grant I P, Johnson C T, Parpia F A and Plummer E P 1989 *Computer Physics Communications* **55** 425
[39] The National Institute of Standards and Technology [DB/OL] http://www.nist.com.gov/.pmla
[40] Kramida A, Ralchenko Y and Reader J 2014 *NIST ASD Team, NIST Atomic Spectra Database* (ver. 5.2) (http://physicsnistgov/asd National Institute of Standards and Technology Gaithersburg,MD)
[41] Cowan R D 1981 *The Theory of Atomic Structure and Spectra* (Berkeley, CA: University of California Press)